PERGAMON

Atmospheric Environment 36 (2002) 1979–1991

ATMOSPHERIC ENVIRONMENT

www.elsevier.com/locate/atmosenv

Aerosol size and chemical characteristics at Mumbai, India, during the INDOEX-IFP (1999)

Chandra Venkataraman*, C. Konda Reddy, Sajni Josson, M. Shekar Reddy

Centre for Environmental Science and Engineering, Indian Institute of Technology, Powai, Mumbai 400 076, India

Received 26 May 2001; accepted 15 January 2002

Abstract

Aerosol size and chemical characteristics govern their optical and radiative effects and their potential for cloud nucleation. This paper reports the size and chemical characteristics of surface aerosols measured at Mumbai during the Indian Ocean Experiment-Intensive Field Phase (INDOEX-IFP), January–March 1999. Carbonaceous (30%) and ionic (20%) constituents contributed significantly to aerosol mass. High black carbon concentrations and a low organic to black carbon ratio implied the predominance of primary carbonaceous aerosol, while a high nss-sulphate contribution in the fine mode, suggested a probable anthropogenic origin. Non-sea-salt potassium (nss-K^+) and black carbon concentrations correlated during January and early February, with nss-K^+ in the fine mode contributing 86% of total-K^+, implying a common origin from a local biomass-burning source. Crustal sources were dominant during late-February and March, with 69% of the aerosol mass present in the coarse mode, and 60% of the variation in PM-10 measured during 12:00–16:00 h being explained by a crustal source factor. Chloride depletion was estimated throughout the study, more significantly during January and early February, from the higher RH and lower Ca^{2+}/Na^{2+} ratios. A negative correlation was obtained of chloride with nitrate, indicating probable nitrate substitution. During late-February and March, nitrate correlated with calcium suggesting an association with soil. Nss-sulphate correlated with calcium but not sodium, implying a probable association with crustal aerosols.

Keywords: PM-10; Aerosol size distributions; BC; OC; Ions; Trace elements

1. Introduction

Tropospheric aerosols and their radiative effects pose a large uncertainty in the evaluation of climate change from anthropogenic modification of the composition of the atmosphere (IPCC, 1996; Haywood and Boucher, 2000). Aerosol radiative effects depend upon aerosol concentration and optical properties, which in turn are governed by their chemical composition and size distribution. Experimental studies of aerosol size and chemical characteristics, along with optical and radiative measurements, are needed to validate and refine calculations of optical and radiative effects. The potential for aerosols to act as cloud condensation nuclei (CCN), and participate in indirect radiative forcing (Charlson et al., 1987), is also governed by their size and chemical characteristics.

Recently, the Indian Ocean Experiment (INDOEX) (Mitra, 1999) was conducted to study feedbacks on climate forcing from anthropogenic and natural aerosols, with the intensive field phase (IFP) of experiments during January–April 1999. Several land-based stations were established (Ahmedabad, Mumbai, New Delhi, Pune, Thiruvananthapuram) for aerosol measurements during the INDOEX-IFP on a concurrent schedule. This paper reports the size and chemical characteristics of surface aerosols measured at Mumbai.

*Corresponding author. Tel.: +91-22-576-7856; fax: +91-22-572-3480.

E-mail address: chandra@cc.iitb.ac.in (C. Venkataraman).

1352-2310/02/$ - see front matter
PII: S1352-2310(02)00167-X

The objectives of this study included the following:

- measuring concentrations of aerosol chemical constituents of climate relevance, including organic carbon (OC), black carbon (BC), ions and trace elements, and selected species size distributions, at the urban/coastal station of Mumbai, during the INDOEX-IFP (January–March 1999),
- evaluating meteorological, atmospheric chemistry and source-contribution effects.

2. Sampling site and particle collection

Mumbai is situated about midway on the western coast of India (19°23′N, 72°50′E) and is a peninsular city joined to the mainland at its northern end (Fig. 1). Large petrochemical, fertiliser and power plants are located to the east and south-east of the city. Several thousand medium and small-scale industries are located in the city including chemical, textile and dyeing, pharmaceutical, paint and pigment and metal-working industries. The land-use pattern is industrial-cum-residential with a total population of over 10 million and a population density of 16,500 persons km^{-2}. Sources of particulate matter in the city include vehicular emissions, power plants, industrial oil burning and refuse burning (Larssen et al., 1997).

Particulate samples were collected on the roof (about 10 m height) of the building of the Centre for Environmental Science and Engineering, at the Indian Institute of Technology Bombay (IITB). This represents a background urban site, about 10 km inland from the coast and likely to receive both marine and continental aerosols. The site is not affected by proximate transportation or industrial sources, with the nearest heavy-traffic roadway about 1 km to the east and industrial cluster about 3 km to the south-east. However, burning of refuse and biomass (leaves, garden-waste) is an intermittent, local source throughout Mumbai, especially at nighttime in winter (December–January). PM-10 samples (mass in particles smaller than 10 μm aerodynamic diameter) were collected using a high-volume sampler (Model PEM, HVF 10, Polltech Instruments, Mumbai), at a flow rate of 1.1 $m^3 min^{-1}$ on quartz fibre filters. A total of seven 24 h average samples were collected on bimonthly schedule, starting 12:00 noon on the sampling days (Table 1). In addition,

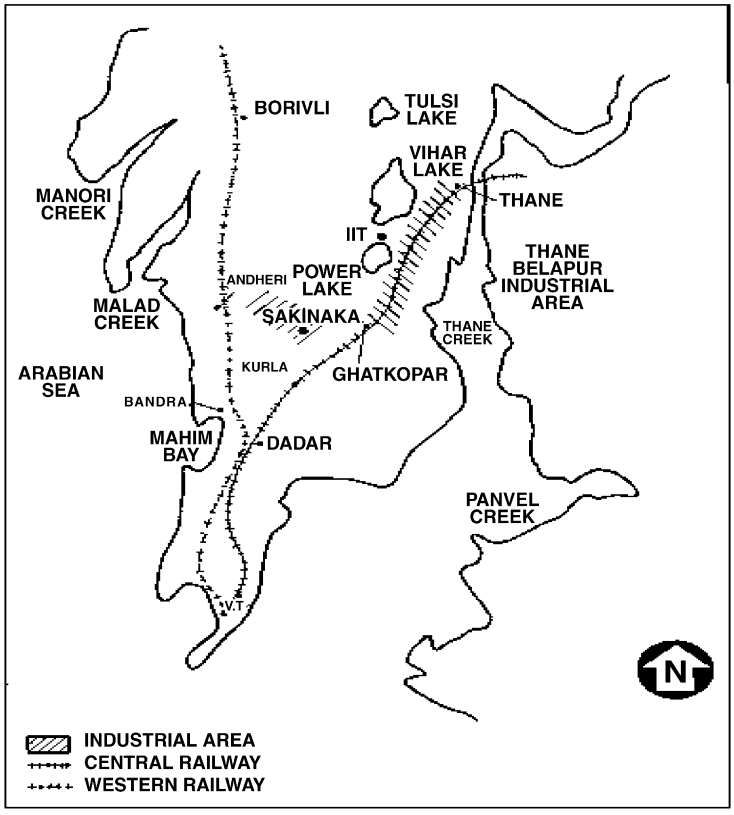

Fig. 1. Location of sampling site at IIT Bombay.

Table 1
Summary of meteorology and aerosol measurements during INDOEX-IFP, 1999

Sampling date	Wind			Temp.(°C)	RH (%)	Mass concentration ($\mu g\,m^{-3}$)	Cloud cover	Remarks
	Speed (ms^{-1})	Direction[a]	Calm (%)					
				Period-1				
40-h Andersen: 12 Jan.	1.4	NE	63	23	60	195	Clear	Air parcels from N,NE continental
19 Jan.	0.9	E	78	25	66	182	Cloudy	Air parcels from E continental
02 Feb.	1.3	NNW	63	27	62	186	Moderate	From central and arid NW India
09 Feb.	1.4	WNW	83	24	62	192	Low cloud	From NW and central India
Average	1.3±0.2		72±10	25±2	62±2	187±6		
24-h PM-10: 13 Jan.	2.6	E,NW	42	28	45	135	Clear	Air parcels from E,NW continental
20 Jan.	1.6	E	75	26	58	232	Cloudy	Air parcels from E continental
10 Feb.	2.1	NW	79	25	79	178	Cloudy	Air parcels from NW marine
Average	2.1±0.5		65±20	26±1	61±17	182±48		
4-h PM-10 5,12 Jan. 4,6,11,22,27, Feb.		E,NW						
Average	1.4±0.6		16±12	29±3	51±20	220±58		
				Period-2				
40-h Andersen: 23 Feb.	2.9	N-NE	60	29	41	159	Clear	From NE, E continental
09 Mar.	3.1	N-NW	50	31	50	132	Clear	Air parcels from NW marine
23 Mar.	2.7	NW	40	32	40	195	Clear	Air parcels from N-NW marine
Average	2.9±0.1		50±10	31±1	44±5	162±31		
24-h PM-10: 24 Feb.	5.4	E,N-NW	58	31	58	163	Low cloud	NW marine and E, N continental air
09 Mar.	2.6	NW	55	32	45	107	Clear	N-NW marine and NW continental
10 Mar.	2.7	N-NW	37	28	37	106	Clear	N-NW marine air
24 Mar.	3.4	NW	46	31	31	138	Clear	NW marine air
Average	3.5±1.3		49±9	30±2	43±12	128±27		
4-h PM-10 Feb. 17,19,26 Mar. 1,3,12,15,19,22,26,29		NW,NNW						
Average	3.0±0.7		7±1	33±1	39±8	246±67		

[a] Predominant wind direction.

twenty-two 4 h average PM-10 samples were collected between 12:00 and 16:00 on a common schedule with other continental groundstations.

Particle size distributions were measured over 40 h average sampling periods using an 8-stage Andersen impactor (Andersen Instruments Inc., USA) with 50%

aerodynamic cut-off diameters of 0.43, 0.65, 1.1, 2.1, 3.3, 4.7, 5.8, 9.0 μm for stages 8 through 1, respectively, with smaller particles collected on an after-filter (Table 1). The impactor, connected to a continuous-duty carbon-vane vacuum pump, operated at a constant air flow-rate of 28.8 $dm^3 min^{-1}$. Quartz fibre-filters (QFFs) backed by aluminium foils were used as impactor substrates. QFFs were used because of their gravimetric stability and inertness towards acidic gases, providing the capability for artefact-free mass and ion measurement (Coutant, 1977; Pierson et al., 1980). The aluminium foil backing ensured particle collection by impaction without particle losses through the filter by filtration which could also lead to a flattening of the impactor efficiency curve (Hering, 1995).

The filters were conditioned for 8 h before and after sampling at about 25°C and 50% relative humidity (RH), and weighed on a microbalance accurate to 10 μg (Model 210B, Sartorius, Germany). A modified Twomey non-linear iterative algorithm (Winklmayr et al., 1990) was used to invert the stage wise mass and ion concentration data. The modes in the inverted size distributions were fitted to log-normal distributions using least-squares error minimisation to estimate the mass median aerodynamic diameter (MMAD), geometric standard deviation (GSD) and the mass fraction in each mode.

3. Chemical analysis

Inorganic ions: Ion chromatography (CDD-6A Ion chromatograph, Shimadzu Corporation, Japan), following water extraction, was used for the analysis of water-soluble inorganic ions including SO_4^{2-}, NO_3^-, Cl^-, Na^+, K^+, Mg^{2+} and Ca^{2+}, in the aerosol samples. Filters were cut, placed in a glass vial, and ultra-sonicated in 10–40 ml of double-distilled water at 40°C for 30 min. The extract was filtered through 0.2 μm pore size Millipore Teflon filters for cleanup. A strongly basic polymethacrylate resin for anions, and a strongly acidic sulphonated polystyrene resin for cations were used. A 50:50 mixture of 2.5 mM phthalic acid and 2.4 mM Tris (hydroxymethyl) aminomethane adjusted to pH 4.0–4.2 at a flow rate of 1.5 $cm^3 min^{-1}$ was used as the mobile phase for anions. The mobile phase used for monovalent cations was 0.625 mM nitric acid and for divalent cations was a 50:50 mixture of 2 mM tartaric acid and 1 mM ethylenediamine. The conductivity detector was calibrated with standard solutions and detection limits for the various ions ranged from 0.002 ppm (for Na^+) to 0.047 ppm (for SO_4^{2-}).

Trace elements: Trace elements were analysed by acid extraction and atomic emission spectroscopy (ICP-AES). A portion of the filter was covered with 5 ml concentrated HCl, 3 ml concentrated HNO_3 and 2 ml concentrated $HClO_4$ and heated to 150–160°C till the solution was clear. ICP-AES (Model 8440, GBC Scientific Equipment, Australia), was used for the analysis of acid soluble fraction of PM-10 aerosols i.e., Al, Si, Fe, Mn, Zn, Cu, Ca, Mg, Ni, Cr, V, As, Co, Sb, Cd and Pb. Detection limits for various elements ranged from 2×10^{-4} ppm for Na^+ to 0.5 ppm for Pb. Among these elements Pb, Cr, V, Co, As, Sb and Cd were below detection limit. Efficiency of recovery by the acid extraction procedure was measured by spiking one half of a particle-laden filter with known amounts of elements. Extraction of both filter halves and analysis gave recoveries of 85–92% for Ca, Mg and Fe and of 77% for Pb, which were used to correct the measured concentrations. The low recovery fraction of Pb is from its low solubility in acid.

Elemental and organic carbon: Carbon analysis was carried out at the Environmental Quality Laboratory, California Institute of Technology, using a thermal-optical method (Turpin et al., 1990). The detection limits for organic carbon (OC) and black carbon (BC), respectively, were 0.2 and 0.1 μg of carbon. Most thermal methods use pyrolysis in He at temperatures of 525–700°C for OC evolution followed by oxidation in air or oxygen at temperatures of 700–950°C for BC evolution (Countess, 1990; Hering et al., 1990). The evolved carbon is estimated as CO_2 using NDIR or reformed and estimated as CH_4 by FID. While total carbon has been estimated to within 20% among various laboratories, significant differences persist in the OC/BC ratio. The variability in the BC estimation can be explained by the analysis methods, while that in the OC depends additionally on sampling artefacts including adsorption of volatile organic compounds on filter substrates (Hering et al., 1990). Some methods use optical transmittance or reflectance along with the carbon thermogram to determine the OC/BC split. The thermal-optical transmittance method used in this study (Turpin et al., 1990; Birch and Cary, 1996; Christoforou et al., 2000), superimposes the laser transmittance, FID signal and oven temperature as a function of time to identify the OC/BC split. As the oven temperature is increased and OC pyrolyses, the initial aerosol sample transmittance decreases. Then the addition of oxygen results in BC oxidation and increase of the laser transmittance to the initial sample transmittance, which is taken as the OC/BC split. The carbon evolved after this point results from oxidation of BC and the laser transmittance increases to its final value.

4. Results and discussion

4.1. Meteorological description

Mumbai has a tropical monsoon climate with diurnal land and sea breezes (Fig. 1) of daytime onshore winds

from the W and NW and nighttime offshore winds from the N, E and NE. Analysis of hourly wind speed and direction data obtained from Indian Meteorological Department (IMD), Mumbai, revealed the features summarised in Table 1.

Period-1, from January to early February had calm days (average of 65–72% time during the sampling periods with wind speed $<0.5\,ms^{-1}$), with occasional cloud cover, low wind speed ($1.3–2.1\,ms^{-1}$), high relative humidity (average 62%), poor visibility and a few rain events. The predominant wind direction in this period was continental from E, NE and NW with high stagnation and poor dispersion potential. Period-2, from mid-February to end-March, had days with higher average wind speeds ($2.9–3.5\,ms^{-1}$), low relative humidity (average 43%), lower incidence of calm (average 50%), bright sunshine, and mostly moderate to good visibility conditions. The predominant wind direction in this period was marine, NW, N-NE, N-NW, showing good dispersion potential. During the 4 h sampling periods (12:00–16:00), wind fluctuations were high in both Period-1 and Period-2. The predominant wind direction in Period-1 was from E, NW with moderate wind speeds ($1.2–2.1\,ms^{-1}$), low frequency of calm (16%) and lower average temperature (29°C). Period-2 had higher average wind speeds ($2.7–3.7\,ms^{-1}$), very low frequency of calm (average of 7% time), and higher average temperature (33°C).

4.2. Particle mass concentrations and size distributions

In Period-1, the particulate mass concentration was high, in both 24 h PM-10 and 40 h Andersen impactor samples, with an average of $182\pm48\,\mu g\,m^{-3}$ and $187\pm6\,\mu g\,m^{-3}$ respectively (Table 1). In Period-2, there were lower concentrations, of $128\pm27\,\mu g\,m^{-3}$ and $162\pm31\,\mu g\,m^{-3}$, respectively, in the 24 h and 40 h average samples. Sampling dates and duration were not the same for 24 h PM-10 and 40 h Andersen samples and the impactor sampling period included 16 h of daytime and 24 h of nighttime while the PM-10 sampling period included 12 h each of daytime and nighttime. However, data from both samplers were used to explain the average aerosol characteristics in Periods 1 and 2.

The high aerosol concentration during Period-1, from January to early February, was associated with low average wind speed ($1.3–2.1\,ms^{-1}$), from easterly industrial areas, and high frequency of calm conditions (65–72%), implying predominant anthropogenic sources, corroborated by the predominant fine fraction (0.64) (Fig. 2a). The decrease in the aerosol concentration in late February was mainly because of increased frequency of winds and greater dispersion (only 50% calm), and its increase in March was because of higher average continental surface wind speeds ($2.7–3.7\,ms^{-1}$, from NW and W), and greater crustal source contribution, corroborated by the predominant coarse fraction (0.69) in Period-2 (Fig. 2a).

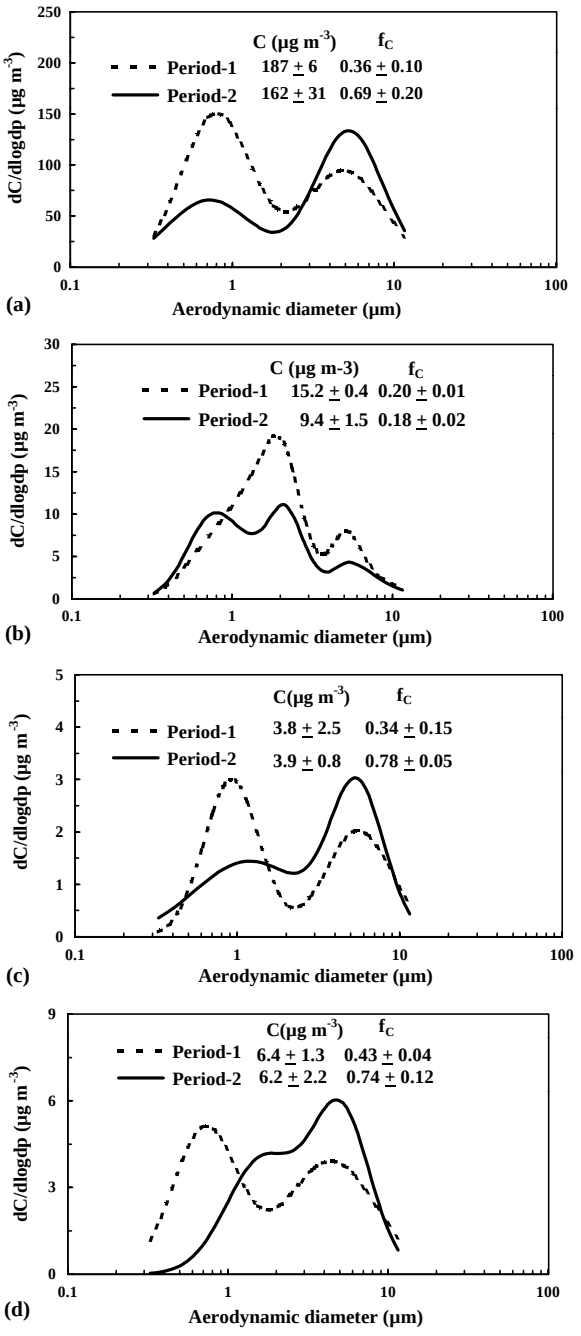

Fig. 2. Size distributions of (a) aerosol mass, and the anions, (b) non-sea-salt sulphate, (c) chloride and (d) nitrate. The coarse mode fraction is denoted by f_c.

The fine fraction increased from 0.46 in early January to 0.60 in early February (Period-1) and then decreased to 0.36 in March (Period-2). The average fine fraction of

Table 2
Average concentrations of 24-h PM-10 and chemical constituents in the two meteorological periods

Species	Period-1		Period-2	
	Concentration ($\mu g\,m^{-3}$)	Contribution (%)	Concentration ($\mu g\,m^{-3}$)	Contribution (%)
PM-10				
High vol. sampler (24-h)	182 ± 48[a]		128 ± 27[a]	
Carbonaceous matter				
Organic carbon (OC)	37.3 ± 10.5	20.5 ± 2.6	25.3 ± 9.9	19.2 ± 3.7
Black carbon (BC)	12.4 ± 5.1	6.6 ± 0.9	12.6 ± 3.0	9.8 ± 2.0
Carbonate carbon	2.5 ± 0.7	1.3 ± 0.2	1.3 ± 0.9	0.9 ± 0.6
OC/BC	3.1 ± 0.5		2.0 ± 0.3	
Total carbon/PM-10	52.2 ± 16.3	28.4 ± 2.6	39.1 ± 13.0	30.0 ± 4.0
Inorganic ions				
$ssSO_4^{2-}$ [b]	0.5 ± 0.2	0.3 ± 0.2	0.7 ± 0.1	0.5 ± 0.2
$nssSO_4^{2-}$ [c]	6.8 ± 2.4	3.8 ± 1.3	5.5 ± 0.9	3.9 ± 1.5
% of total SO_4^{2-}	93.1 ± 5.2		88.7 ± 3.0	
NO_3^-	4.7 ± 1.7	2.8 ± 1.7	6.0 ± 3.0	4.8 ± 2.7
Cl^-	0.8 ± 0.2	0.4 ± 0.1	2.6 ± 1.8	2.1 ± 1.5
Na^+	2.0 ± 0.6	1.2 ± 0.7	2.2 ± 0.9	1.6 ± 0.8
K^+	13.2 ± 2.8	7.4 ± 0.4	8.9 ± 2.5	6.1 ± 1.6
Mg^{2+}	1.4 ± 0.9	0.7 ± 0.2	2.2 ± 3.4	1.1 ± 1.4
Ca^{2+}	3.2 ± 1.3	1.8 ± 0.7	6.2 ± 10.9	2.8 ± 4.3
Σ^+ [d] $/\Sigma^-$ [e]	2.8 ± 0.7		2.4 ± 2.0	
Total ions/PM-10	32.6 ± 3.7	18.6 ± 3.5	34.1 ± 21.8	21.9 ± 8.8
Elements				
Al	3.33 ± 0.83	2.0 ± 1.0	1.89 ± 0.68	1.5 ± 0.4
Si	0.07 ± 0.04	0.1 ± 0.0	0.05 ± 0.04	0.5 ± 0.0
Fe	1.92 ± 0.95	1.1 ± 0.6	2.32 ± 0.90	2.0 ± 0.3
Mn	0.04 ± 0.02	0.0 ± 0.0	0.15 ± 0.02	0.1 ± 0.0
Zn	0.77 ± 0.43	0.5 ± 0.4	0.35 ± 0.25	0.2 ± 0.1
Total elements/PM-10	6.16 ± 0.43	3.6 ± 0.4	4.70 ± 0.39	3.6 ± 0.2
Unexplained	90.60 ± 7.87	49.7 ± 12.6	50.18 ± 10.05	39.0 ± 14.5

[a] Mean $\pm$ 1 standard deviation of 3 samples in Period-1 and 4 samples in Period-2.
[b] Sea-salt.
[c] Non-sea-salt.
[d] Sum of cations in $neq\,m^{-3}$.
[e] Sum of anions in $neq\,m^{-3}$.

Mumbai aerosol (0.47) was lower than that reported from other urban locations, e.g., Boston, Long Beach and Hong Kong (0.62–0.68) (Chow et al., 1994a, b; Zhuang et al., 1999a, b). This indicates the relative predominance of the coarse particles at Mumbai, consistent with surface wind characteristics. In both periods, the 4 h average PM-10 concentrations (12:00–16:00) were higher than the respective 24 h average values (Table 1). These were 165–215 $\mu g\,m^{-3}$ in Period-1 and 146–307 $\mu g\,m^{-3}$ in Period-2, with the higher values being more prominent in the latter period, associated with higher wind speeds (2.7–3.7 ms^{-1}) from W and NW. This implies that the afternoon aerosol load was likely from wind blown constituents like dust and sea-salt.

4.3. Chemical composition of PM-10 aerosols

The 24 h PM-10 aerosol samples showed that the measured chemical constituents including carbonaceous, ionic and elemental species accounted for 50–60% of the PM-10 mass, leaving about 40–50% unexplained (Table 2). Carbonaceous species were major contributors (30%) followed by water-soluble ions (20%) and trace elements (4%). The composition of the unexplained mass cannot be determined based on the present study, but has been shown to contain chemical species including ammonium ion, hydrogen and oxygen associated with minerals and organic matter in previous studies seeking a chemical mass balance of particulate matter (e.g. Chow et al., 1994b).

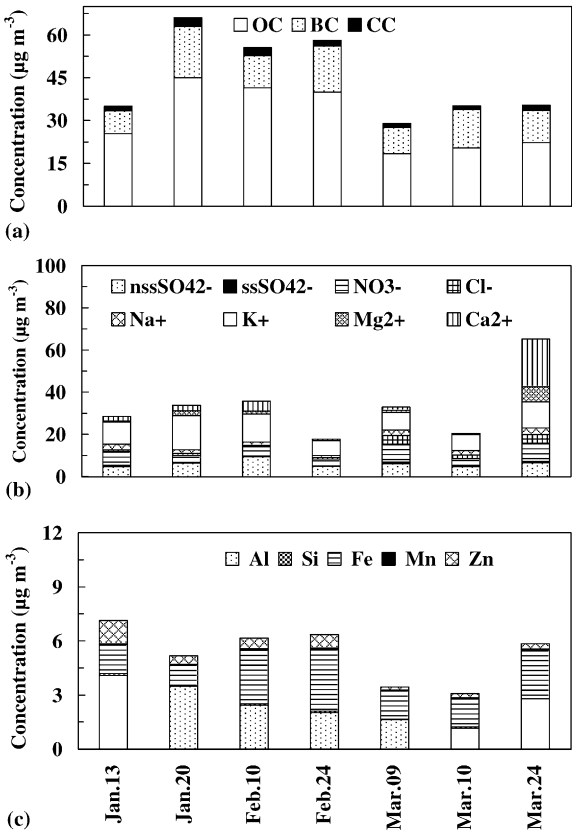

Fig. 3. Concentrations of (a) carbonaceous species (b) ions and (c) elements, in the 24 h average PM-10 samples.

4.3.1. Carbonaceous constituents

Carbonaceous aerosols (OC, BC and carbonate carbon) concentrations were somewhat higher in Period-1 ($52.2 \pm 16.3\,\mu g\,m^{-3}$) compared to Period-2 ($39.1 \pm 13.0\,\mu g\,m^{-3}$) (Table 2) and contributed about 30% of the PM-10 mass. The ratio of concentrations of OC to BC (OC/BC) showed a higher OC/BC ratio of 3.1 in Period-1 compared to 2.0 in Period-2, consistent with stagnation conditions leading to possible formation of secondary organic aerosol from photochemical gas-to-particle conversion of gas-phase organics. This is also borne out for individual sampling days (Fig. 3a).

The OC/BC ratio has been used to explain the possible formation of secondary OC aerosols in the atmosphere (Turpin et al., 1991). While, OC may be primary or secondary in origin, BC is a primary pollutant and OC/BC ratios greater than 1.2–2.4 indicate possible secondary OC formation (Turpin et al., 1991). The relative predominance of primary carbonaceous aerosol in Mumbai, is indicated from the lower OC/BC ratios of 2.0–3.1 measured here and from the higher OC/BC ratios (Burbank 4.1, Los Angeles 3.6, Long Beach 3.2, Pasadena 4.8), reported in other urban airsheds, using the same OC/BC measurement method as in this work (Chow et al., 1994a, b; Turpin et al., 1991; Turpin and Huntzicker, 1991).

4.3.2. Inorganic ions

The concentrations of Na^+ in Period-1 and Period-2 were similar (2.0–2.2 $\mu g\,m^{-3}$), but the Cl^- concentration in Period-2 ($2.6 \pm 1.8\,\mu g\,m^{-3}$) was higher than in Period-1 ($0.8 \pm 0.2\,\mu g\,m^{-3}$) (Table 2 and Fig. 3b). The size distributions of both Cl^- and Na^+ were predominant in coarse particles in Period-2 (Figs. 2c and 4a) implying a predominance of coarse sea-salt particles in this period consistent with the higher average onshore wind speeds from the NW.

Among the anionic components, sulphate was the major contributor (4%) to total PM-10 mass (Table 2 and Fig. 3b). The concentration of non-sea-salt or nss-sulphate was calculated by subtracting sea-salt sulphate from total sulphate by assuming a sulphate to sodium mass ratio in seawater of 0.2516 (Savoie et al., 1987; Cheng et al., 2000). nss-Sulphate contributed predominantly (93% and 89%, respectively, in Periods 1 and 2) to the total sulphate concentrations. The nss-sulphate size distribution in Period-1 was bimodal and in Period-2 was trimodal (Fig. 2b) with a fine fraction of over 80% in both periods suggesting an anthropogenic origin from gas-to-particle conversion of industrial SO_2 emissions significant in this air basin (Venkataraman et al., 2001). This study did not examine the contributions of natural sources of non-sea-salt sulphate like DMS and MSA.

Bimodal sulphate size distributions, similar to those in Period-1, have been previously measured at this site (Venkataraman et al., 2001) during periods of high calm and low wind speeds, with high potential for gas-to-particle conversion of industrial SO_2 emitted in this air basin. Trimodal sulphate size distributions, similar to those in Period-2, were also measured in the previous study, during periods of steady, S/SW onshore winds, with infrequent calm conditions, implying an association with sea-salt. This is further corroborated in the present study, by the higher average wind speeds from the S/SW in Period-2, and the larger average Na^+ concentrations, especially in the coarse mode in this period.

High potassium concentrations were measured, especially in Period-1, ($13.2 \pm 2.8\,\mu g\,m^{-3}$) but also in Period-2 ($8.9 \pm 2.5\,\mu g\,m^{-3}$) (Table 2 and Fig. 3b). The potassium size distributions (Fig. 4b) were bimodal and had a fine fraction predominance (over 85%) in Period-1 (indicating a biomass burning or vegetative origin), but a coarse fraction predominance in Period-2 (possible sea-salt association). Non-sea-salt-K^+ was estimated using a $[K^+]/[Na^+]$ molar ratio of 0.037 in sea water (Cheng et al., 2000). nss-K^+ was estimated as the difference between total-K^+ and that associated with sea-salt estimated as the ratio times the Na^+

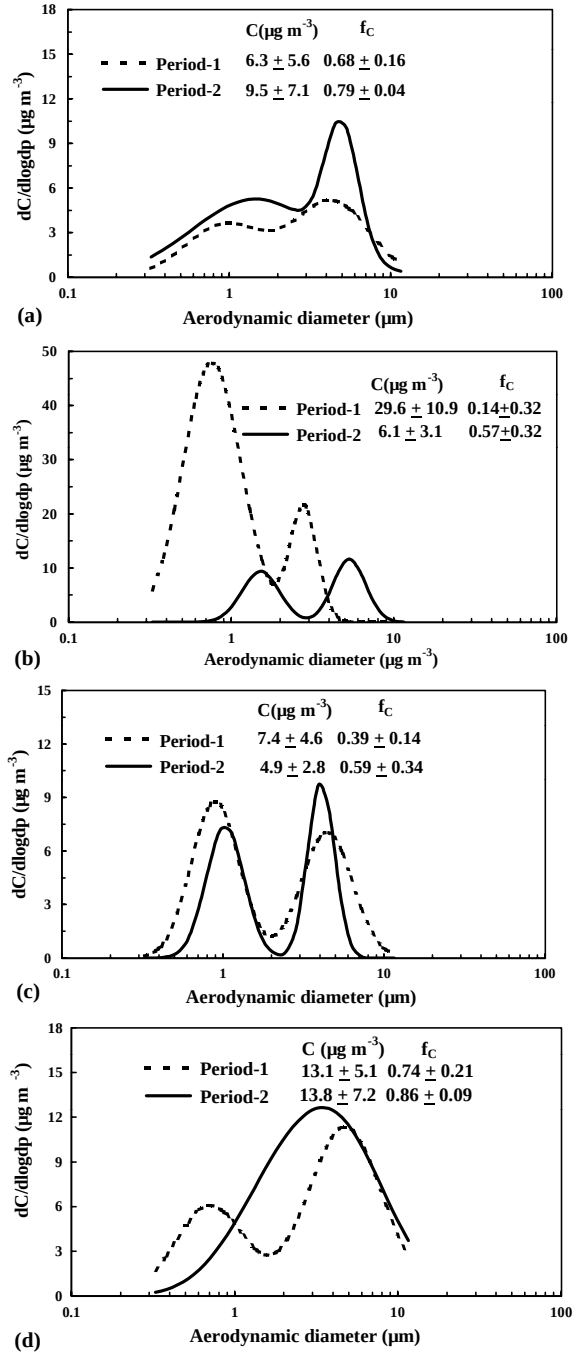

Fig. 4. Size distributions of the cations, (a) sodium, (b) potassium, (c) magnesium and (d) calcium. The coarse mode fraction is denoted by f_c.

concentration. nss-K^+ was predominant in both periods, contributing 99% of total K^+ in Period-1, in both the 24 h PM-10 and 40 h impactor samples. In Period-2 nss-K^+ was 98% of total-K^+ in the 24 h PM-10 and 90% in the 40 h impactor samples. Modal contributions in the impactor samples showed fine fraction nss-K^+ was 86% of total-K^+ in Period-1, when nighttime local biomass burning was noticed, while it was only 32% in Period-2, when this source was not active. In the coarse mode of the impactor samples, sea-salt-K^+ was 1% of total-K^+ in Period-1, but 8% in Period-2, when higher average wind speeds resulted in a greater predominance of coarse mode sea-salt, as corroborated by the large coarse mode Na^+ peak in this period.

The concentrations of nitrate aerosol were similar in both periods (4.7–6.0 $\mu g\,m^{-3}$) (Table 2 and Fig. 3b). Nitrate size distributions however showed a clear submicron peak in Period-1, but a higher average diameter of the fine mode in Period-2 (Fig. 2d).

The concentrations of Ca^{2+} and Mg^{2+} were higher in Period-2 (6.2 and 2.2 $\mu g\,m^{-3}$) than in Period-1 (3.2 and 1.4 $\mu g\,m^{-3}$) (Table 2), because of higher average wind speeds (2.7–3.4 ms^{-1}) contributing soil and re-suspended dust. On the last sampling date of 24 March, the significantly higher cation concentrations (Fig. 3b) resulted from the high wind speed of 3.4 ms^{-1} indicating a high crustal source contribution. While Mg^{2+} showed a modest predominance in the coarse mode in Period-2 (Fig. 4c), Ca^{2+} showed a significant coarse mode peak (Fig. 4d) with a negligible fine fraction, consistent with the association of Ca^{2+} and Mg^{2+} with coarse, crustal particles. Previous studies of aerosols in the Indian region at urban, continental and coastal sites have shown an overall alkaline nature, with a predominance of cations over anions (Sharma and Patil, 1992a, b; Saxena et al., 1996; Momin et al., 1999; Parmar et al., 2001).

4.3.3. Trace elements

Trace element concentrations in 24 h PM-10 samples were similar in both periods (Table 2) and contributed about 3% of the PM-10 mass. Lead was below detection limit (0.5 ppm or 0.04 $\mu g\,m^{-3}$) in all samples (Fig. 3c). The trace element concentrations in the 4 h PM-10 samples were significantly higher (75%) than those in the 24 h PM-10 samples. This was caused mainly by the higher concentrations of crustal trace elements in the 12:00–16:00 sampling periods when higher average wind speeds resulted in greater wind blown dust contributions.

4.4. Chloride loss from sea-salt particles by reactions of nitrate and nss-sulphate

Several recent studies, using bulk and single particle analysis, have shown that coarse mode nitrate is mainly formed by the reaction of HNO_3 with sea-salt particles, especially when marine aerosol and polluted urban air masses mix together (Zhuang et al., 1999a, b; Zhang et al., 2000; Cheng et al., 2000). Chloride depletion in

sea-salt particles has been explained by the reaction of gases or aqueous HNO_3 or H_2SO_4 with NaCl in sea-salt particles or by the absorption of gaseous SO_2 by sea-salt droplets later oxidised to sulphuric acid (Harrison and Pio, 1983; Wall et al., 1988; Mamane and Gottlieb, 1992).

Assuming that all chloride was from sea-salt, and a molar ratio of $[Cl^-]_{original}$ to $[Na^+]$ in sea-salt of 1.174 (Zhuang et al., 1999b), the percent chloride depletion, on a molar basis, was calculated as

$$Cl^-_{depletion}(\%) = [(1.174 * Na^+) - (Cl^-_{measured})]/(1.174 * Na^+) * 100\%. \quad (1)$$

The measured ratio of Cl^- to Na^+ in both Period-1 and 2 was less than that in seawater (Table 3) showing chloride depletion in both periods. The percentage chloride depletion was higher in Period-1 (about 78%), than in Period-2 (about 40%) (Table 3).

In order to examine the potential role of nitrate and nss-SO_4^{2-} in Cl^- depletion, a correlation was sought of NO_3^- and nss-SO_4^{2-} with Cl^-. While there was no correlation between nss-sulphate and Cl^-, an anti-correlation was obtained between nitrate and Cl^- (R^2 of 0.77), especially in the coarse mode (R^2 of 0.98). This implies that Cl^- loss was related to nitrate formation, but not to nss-sulphate formation on sea-salt particles. In addition, a good correlation was obtained for Na^+ with NO_3^-, for both Period-1 (R^2 of 0.73) and Period-2 (R^2 of 0.64), but not with nss-sulphate, corroborating the association of nitrate, but not of nss-SO_4^{2-}, with sea-salt particles.

Nitrate formation on sea-salt particles was seen to depend upon both relative humidity and the relative abundance of Ca^{2+} and Na^+ (competition between Ca^{2+} and Na^+ for acidic gases) (Zhuang et al., 1999b). In this study, the higher Cl^- depletion in Period-1 can be attributed to the low Ca^{2+}/Na^+ ratios (average of 3.3, implying high Na^+ concentrations) and high relative humidity (62%) observed in this period (Table 3). The extent of chloride depletion from the nitrate reaction was found to be larger on fine fraction particles (Fig. 5). It has been suggested that the depletion reaction would favour smaller particles because of their larger total surface area and longer atmospheric residence time (Pakkanen, 1996; Zhuang et al., 1999a). The depletion decreased with increasing particle size and was especially low on coarse fraction particles in Period-2 (Figs. 5 and 6). This can be attributed to the higher coarse mode Ca^{2+}/Na^+ ratio in Period-2 (Table 3), resulting in a preferential uptake of the nitrate by Ca^{2+} rather than by Na^+ containing particles.

4.5. Reactions of nitrate and nss-sulphate on soil particles

HNO_3, H_2SO_4 and SO_2 can also react with carbonates such as $CaCO_3$ and $MgCO_3$ on soil particles to form coarse nitrate and sulphate (Harrison and Pio, 1983; Wall et al., 1988; Mamane and Gottlieb, 1992; Zhuang et al., 1999a). The nitrate which replaced chloride in sea-salt particles was estimated on an equivalent basis and subtracted from total measured nitrate to give the nitrate

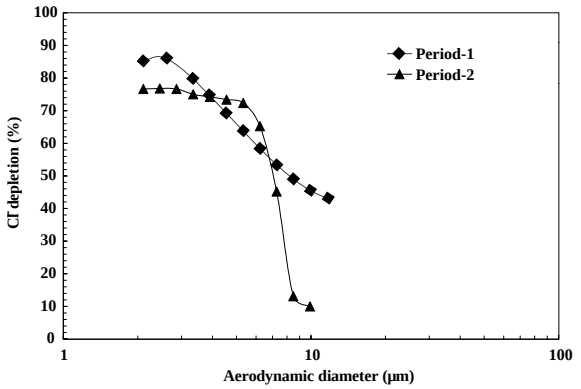

Fig. 5. Chloride depletion as a function of particle size for Period-1 and Period-2.

Table 3
Equivalent ratios of Cl^- and Ca^{2+} to Na^+, percent chloride depletion, and nitrate associated with soil ($NO_{3\,soil}^-$) during Period-1 and Period-2

Period	Number of samples (n)	Cl^-/Na^+	Ca^{2+}/Na^+	Cl^- depletion (%)	$NO_{3\,soil}^-$ (neq m^{-3})	$NO_{3\,soil}^-$ (%)
Period-1						
40-h Andersen	4	0.61±0.56	4.35±2.78	72±9	Nil	
24-h PM-10	3	0.26±0.12	2.01±1.00	78±11	Nil	
Period-2						
40-h Andersen	3	0.72±0.52	6.32±2.30	59±39	90.1±11.5	95±5
24-h PM-10	4	0.71±0.27	2.51±0.68	39±24	85.1±10.2	69±20
Sea water		1.17[a]	0.04[a]			

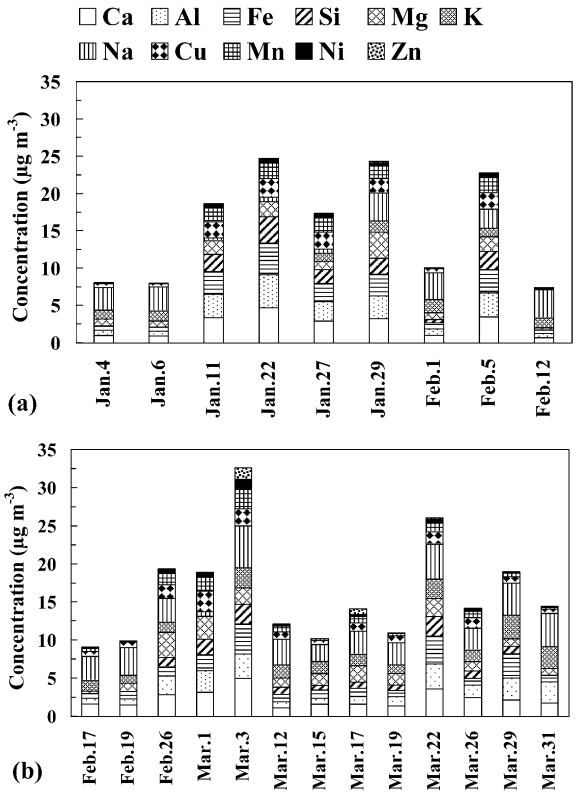

Fig. 6. Concentrations of trace elements in 4 h average PM-10 samples during (a) Period-1 and (b) Period-2.

available for association with soil particles ($[NO_3^-]_{soil}$). This assumes that chloride depletion is only from the nitrate reaction, consistent in this study with the absence of any correlation of Na^+ or Cl^- with nss-sulphate.

$$[NO_3^-]_{soil} = [NO_3^-]_{total} - (1.174 * Na^+ - Cl^-). \quad (2)$$

No nitrate was available for reaction with soil in Period-1, while significant nitrate was associated with soil in Period-2 (Table 3). A good correlation (R^2 of 0.70) was obtained between $NO_{3\,soil}^-$ and Ca^{2+} in Period-2. The coarse mode predominance of nitrate in Period-2 (Fig. 2d), but not in Period-1, also supports its association with soil particles.

A good correlation was obtained between non-sea-salt sulphate and calcium in total particles for both periods (R^2 of 0.87 and 0.89) and in the coarse mode in Period-1 (R^2 of 0.84), implying nss-sulphate association with soil particles containing Ca^{2+}.

4.6. Qualitative source resolution

4.6.1. Lead concentrations

In the present study, Pb concentrations were below detection limit (0.5 ppm or 0.04 μg m^{-3}) in all collected samples. The supply of unleaded petrol was started in Mumbai in April 1995, with a complete phase-out of leaded petrol by October 1999. Lead concentrations in Mumbai ranged 0.46–1.39 μg m^{-3} to 0.20–0.68 μg m^{-3} in the years 1988–1994 (Table 4), with a previous measurement of 0.55 μg m^{-3} in 1989 at the same site (Sharma and Patil, 1992a,b), and its reduction is likely from the recent introduction of unleaded petrol.

Table 4
Summary of Pb concentrations at residential/industrial sites in Mumbai

Site	Year	Concentration (μg m^{-3})
Various sites	1988–89	0.46–1.39[a,b]
Various sites	1992–94	0.21–0.68[a]
CESE, IIT Bombay	1989	0.41–0.71[b]
CESE, IIT Bombay (This study)	1999	BDL (<0.04)

[a] Tripathi (1998).
[b] Sharma and Patil (1992a, b).
BDL: below detection limit.

4.6.2. Potassium and black carbon

Biomass burning contributes to both BC and potassium emissions (Penner, 1995; Cooper and Watson, 1980). In addition, vegetation has been proposed as another source of K^+ particles (Kleinman et al., 1979) emitted by respiration through stomata. While K^+ concentrations were high in both periods in PM-10 samples (Table 2), the Andersen impactor samples showed much higher K^+ concentrations in Period-1 (Fig. 4b) with a major peak in the fine mode. In addition, a good correlation was obtained between nss-K^+ and BC in Period-1 (R^2 of 0.96). Open burning of dry leaves and garden-waste, especially during nighttime, has been observed in the IIT-Bombay campus in this period, making this the likely source of both pollutants. Refuse burning in Mumbai has been estimated to contribute about 23% of the PM-10 emissions in this basin (Larssen et al., 1997). The Andersen impactor sampling period of 40 h included 16 h of daytime and 24 h of nighttime sampling, when biomass burning activities predominate, showing the effect of this source in Period-1.

4.6.3. Principle component analysis

Trace element concentrations in the 4 h PM-10 samples (Fig. 6) were also used to explain sources. As the 4 h PM-10 samples were large enough in number (22) for multivariate analysis, principal component analysis (SPSS/PC+ V3.0, SPSS Inc., 1988) was attempted to identify the possible sources, using the elemental analysis (eleven elements) and meteorological parameters (wind speed (WS), %RH, and %calm). Four

Table 5
Factor loadings of the concentrations of 4-h PM-10 and constituent trace elements (Varimax rotated factor pattern)

Variable	FACTOR 1	FACTOR 2	FACTOR 3	FACTOR 4	Communality
PM-10	**0.70**	0.52	0.24	0.38	0.97
WS[a]	**0.83**	0.38	0.29	0.19	0.96
RH[b]	−0.72		**−0.63**		0.92
Temp.	0.25	0.14	**0.83**	0.23	0.92
Calm	0.07			−0.92	
Ca^{2+}	**0.87**	0.37	0.22	0.12	0.97
Al	**0.93**	0.06	0.27	−0.12	0.96
Fe	**0.89**	0.21	0.07	0.34	0.97
Si	**0.92**	0.17	0.23	0.21	0.98
Mg^{2+}	0.31	0.02	**0.88**	−0.07	0.95
K^+	0.40	0.51	0.17	**0.70**	0.99
Na^+	0.14	0.59	0.37	**0.62**	0.94
Cu	**0.91**	0.15	0.17	−0.26	0.97
Mn	**0.86**	0.34	0.17	−0.22	0.95
Ni	0.65	**0.70**	0.09		0.95
Zn	0.26	**0.93**		0.04	0.96
Eigenvalue	10.28	2.45	1.54	1.21	
% of variance	60.5	14.4	9.1	7.1	

[a] WS: wind speed.
[b] RH: relative humidity.

factors were found explaining 91.1% of total variance (Table 5).

FACTOR 1, explaining 60.5% of the variance, had high loadings of PM-10, Ca, Al, Fe, Si, Cu and Mn with wind speed. PM-10 mass correlated with wind speed and crustal elements (Ca, Al, Fe and Si) implying re-suspension of soil particles as a main contributor to the PM-10 mass in the afternoon period. This factor also had high loadings for Cu and Mn, which are generally from non-ferrous industrial emissions. Thus, FACTOR 1 represents crustal source contaminated by industrial emissions. FACTOR 2 included Ni and Zn, accounting for 14.4% of the variance, and may be from pollution sources like oil and refuse burning. FACTOR 3, explaining 9.1% of the variance, has high loading of Mg^{2+} with temperature (Temp), but could not be identified with regard to source. FACTOR 4, accounting 7.1% of the variance, had high loading of Na^+, K^+ and strongly anti-correlated with calm conditions (Calm), representing the marine source. Steady, onshore winds from the sea during the afternoon period resulted in low occurrence of calm conditions, and the possible contribution of Na^+ and K^+ associated with sea-salt aerosol.

5. Conclusions

The aerosol in Mumbai during the INDOEX-IFP contained significant amounts of carbonaceous (30%) and ionic (20%) constituents. The composition of the unexplained 50% balance mass has not been determined in this work, but has been shown in previous studies to contain NH_4^+ ion and constituents including oxygen and hydrogen, associated with minerals and organic matter. A low OC/BC fraction revealed the relative predominance of primary carbonaceous aerosol, and a high nss-sulphate contribution, especially in the fine mode, pointed to anthropogenic origin of the sulphate. High potassium and BC concentrations in January to early February were likely from a local biomass-burning source. Crustal sources dominated the aerosol during late-Feb and March, especially in the afternoon (12:00–16:00) period.

Chloride depletion, likely from the nitrate reaction, was estimated throughout the study, and was predominant in Jan to early Feb from the higher RH and lower Ca^{2+}/Na^+ ratios. In late-Feb to March, significant nitrate was associated with soils as evidenced by the correlation of balance-nitrate with calcium. nss-Sulphate did not correlate with sodium, but showed a significant correlation with calcium throughout the study, suggesting association with crustal sources rather than sea-salt.

While the measurements point to natural sources like sea-salt and crustal aerosol, the high concentrations of nss-sulphate and black carbon indicate an anthropogenic contribution. The strong urban pollution signal makes it difficult to assess the contribution of synpotic scale or regional scale processes to the aerosol measured over Mumbai during the INDOEX-IFP. The

predominance of inorganic ions and organic carbon (a fraction of which would be hygroscopic), indicate that these aerosols could act as potential cloud condensation nuclei (CCN).

Acknowledgements

We thank Glen Cass (Georgia Institute of Technology, USA) and Lynn Salmon (California Institute of Technology, USA) for generously supplying the carbon analysis of the PM-10 samples. We acknowledge the contributions of Tarun Gupta and Suresh Varghese (IIT, Bombay) to this work. We gratefully acknowledge the assistance of Gauri Pandit (Bhabha Atomic Research Centre, Mumbai) with ion chromatography methods and Vinod Kumar (Bhabha Atomic Research Centre, Mumbai) with principal component analysis.

References

Birch, M.E., Cary, R.A., 1996. Elemental carbon-based method for monitoring occupational exposures to particulate diesel exhaust. Aerosol Science and Technology 25, 221–241.

Charlson, R.J., Lovelock, J.S., Andreae, M.O., Warren, S.G., 1987. Oceanic phytoplankton, atmospheric sulphur, cloud albedo and climate. Nature 326, 655–661.

Cheng, Z.L., Lam, K.S., Chan, L.Y., Wang, T., Cheng, .K.K., 2000. Chemical characteristics of aerosols at coastal station in Hong Kong. I. Seasonal variation of major ions, halogens and mineral dusts between 1995 and 1996. Atmospheric Environment 34, 2771–2783.

Christoforou, C.S., Salmon, L.G., Hannigan, M.P., Solomon, P.A., Cass, G.R., 2000. Trends in fine particle concentration and chemical composition in Southern California. Journal of Air and Waste Management Association 50, 43–53.

Chow, J.C., Watson, J.G., Fujita, E.M., Lu, Z., Lawson, D.R., Ashbaugh, L.L., 1994a. Temporal and spatial variations of PM-10 and PM-2.5 aerosol in the Southern California Air Quality study. Atmospheric Environment 28 (12), 2061–2080.

Chow, J.C., Watson, J.G., Fujita, E.M., Lu, Z., Lawson, D.R., Ashbaugh, L.L., 1994b. Chemical mass balance source apportionment of PM-10 during the Southern California Air Quality study. Aerosol Science and Technology 21, 1–36.

Cooper, J.A., Watson, J.G., 1980. Receptor oriented methods of air particulate source apportionment. Journal of Air Pollution Control Association 30 (10), 1116–1125.

Countess, R.J., 1990. Interlaboratory analyses of carbonaceous aerosol samples. Aerosol Science and Technology 12, 114–121.

Coutant, R.W., 1977. Effect of environmental variables on collection of atmospheric sulphate. Environmental Science and Technology 11, 873.

Harrison, R.M., Pio, A.P., 1983. Size-differentiated composition of inorganic atmospheric aerosols of both marine and polluted continental origin. Atmospheric Environment 17 (9), 1733–1738.

Haywood, J., Boucher, O., 2000. Estimates of the direct and indirect radiative forcing due to tropospheric aerosols: a review. Reviews of Geophysics 38 (4), 513–543.

Hering, S.V., 1995. Impactors, cyclones, and other inertial and gravitational collectors. In: Cohen, B.S., Hering, S.V. (Eds.), Air Sampling Instruments for Evaluation of Atmospheric Contaminants, 8th Edition. American Conference of Governmental Industrial Hygienists, Cincinatti, OH, pp. 279–322.

Hering, S.V., Appel, B.R., Cheng, W., Salaymeh, F., Cadle, S.H., Mulawa, P.A., Cahill, T.A., Eldred, R.A., Surovik, M., Fitz, D., Howes, J.E., Knapp, K.T., Stockburger, L., Turpin, B.J., Huntzicker, J.J., Zhang, X.Q., McMurry, P.H., 1990. Comparison of sampling methods for carbonaceous aerosols in ambient air. Aerosol Science and Technology 12, 200–213.

Intergovernmental Panel on Climate Change, 1996. In: Houghton, et al., J.T. (Eds.), Climate Change 1995: The Science of Climate Change, The Contribution of Working Group I to the Second Assessment Report of the IPCC. Cambridge University Press, New York, 572pp.

Kleinman, M.T., Tomezyk, C., Leaderer, B.P., Tanner, R.L., 1979. Inorganic nitrogen compounds in New York City Air. Annals of the New York Academy of Sciences 322, 115–123.

Larssen, S., Gram, F., Hagen, L.O., Jansen, H., Olsthoorn, X., Aundhe, R.V., Joglekar, U., 1997. In: Shah, J., Nagpal, T. (Eds.), URBAIR—Urban Air Quality Management Strategy in Asia: Greater Mumbai Report. The International Bank of Reconstruction and Development, The World Bank, Washington DC, 231pp.

Mamane, Y., Gottlieb, J., 1992. Nitrate formation on sea-salt and mineral particles—a single particle approach. Atmospheric Environment 26A, 1763–1769.

Mitra, A.P., 1999. INDOEX (India)—introductory note. Current Science 76 (7), 886–889.

Momin, G.A., Rao, P.S.P., Safai, P.D., Ali, K., Naik, M.S., Pillai, A.G., 1999. Atmospheric aerosol characteristics at Pune and Thiruvanathapuram during the INDOEX programme, 1998. Current Science 76 (7), 985–989.

Pakkanen, T.A., 1996. Study of formation of coarse particle nitrate aerosol. Atmospheric Environment 30, 2475–2482.

Parmar, R.S., Satsangi, G.S., Kumari, M., Lakhani, A., Sivastava, S.S., Prakash, S., 2001. Study of size distribution of atmospheric aerosol at Agra. Atmospheric Environment 35, 693–702.

Penner, J.E., 1995. Carbonaceous aerosols influencing atmospheric radiation: black carbon and organic carbon. In: Charlson, R.J., Heintzenberg, J. (Eds.), Aerosol Forcing of Climate. Wiley, England, pp. 91–108.

Pierson, W.R., Wanda, W.B., Thomas, J.K., Timothy, J.T., James, W.B., 1980. Artefact formation of sulphate, nitrate, hydrogen ion on backup filters. Journal of Air Pollution Control Association 30, 31–35.

Savoie, D.L., Prospero, J.M., Nees, R.T., 1987. Washout ratios of nitrate, non-sea-salt sulphate and sea-salt on Virginia key, Florida and on American Samoa. Atmospheric Environment 21, 103–112.

Saxena, A., Kulshrestha, U.C., Kumar, N., Kumari, K.M., Prakash, S., Sivastava, S.S., 1996. Characterization of

precipitation at Agra. Atmospheric Environment 30 (20), 3405.

Sharma, V.K., Patil, R.S., 1992a. Chemical composition and source identification of Bombay aerosol. Environmental Technology 13, 1043–1045.

Sharma, V.K., Patil, R.S., 1992b. Size distribution of atmospheric aerosols and their source identification using factor analysis in Bombay, India. Atmospheric Environment 26B, 135–140.

SPSS, 1988. Manual: Advanced Statistics Manual SPSS/PC+ V 3.0; SPSS Inc., 444 North Michigan Avenue, Chicago IL 60611.

Tripathi, R.M., 1998. Electro-analytical techniques for chemical characterisation of atmospheric aerosols. Indian Aerosol Science and Technology Association (IASTA) 11 (1), 24–36.

Turpin, B.J., Huntzicker, J.J., 1991. Secondary formation of organic aerosols in the Los Angeles Basin: a descriptive analysis of organic and elemental carbon concentrations. Atmospheric Environment 25A (2), 207–215.

Turpin, B.J., Cary, R.A., Huntzicker, J.J., 1990. An in situ, time resolved analyzer for aerosol organic and elemental carbon. Aerosol Science and Technology 12, 161–171.

Turpin, B.J., Huntzicker, J.J., Larson, S.M., Cass, G.R., 1991. Los Angeles summer midday particulate carbon: primary and secondary aerosol. Environmental Science and Technology 25, 1788–1793.

Venkataraman, C., Sinha, P., Bammi, S., 2001. Sulphate aerosol size distributions at Mumbai, India, during the INDOEX-FFP (1998). Atmospheric Environment 35, 2647–2655.

Wall, S.M., John, W., Ondo, J.L., 1988. Measurement of aerosol size distributions for nitrate and major ionic species. Atmospheric Environment 22 (8), 1649–1656.

Winklmayr, W., Wang, H.-C., John, W., 1990. Adaptation of the Twomey algorithm to the inversion of cascade impactor data. Aerosol Science and Technology 13, 322–331.

Zhang, D., Shi, G., Iwasaka, Y., Hu, M., 2000. Mixture of sulphate and nitrate in coastal atmospheric aerosols: individual particle studies in Qingdao, China. Atmospheric Environment 34, 2669–2679.

Zhuang, H., Chan, C.K., Fang, M., Wexler, A.S., 1999a. Size distributions of particulate sulphate, nitrate and ammonium at a coastal site in Hong Kong. Atmospheric Environment 33, 843–853.

Zhuang, H., Chan, C.K., Fang, M., Wexler, A.S., 1999b. Formation of nitrate and non-sea-salt sulphate on coarse particles. Atmospheric Environment 33, 4223–4233.